

NORDITA 97/10 N,P
UAB-FT-97/411
hep-ph/9702302

**CHIRAL-LOOP AND VECTOR-MESON CONTRIBUTIONS
TO $\eta \rightarrow \pi\pi\gamma\gamma$ DECAYS**

LL. AMETLLER^a, J. BIJNENS^b, A. BRAMON^c and P. TALAVERA^b

^a Departament de Física i Enginyeria Nuclear,
Universitat Politècnica de Catalunya, 08034 Barcelona, Spain

^b NORDITA, Blegdamsvej 17, DK 2100 Copenhagen, Denmark

^c Departament de Física, Universitat Autònoma de Barcelona,
08193 Bellaterra (Barcelona), Spain

ABSTRACT

The process $\eta \rightarrow \pi^0\pi^0\gamma\gamma$ is discussed in Chiral Perturbation Theory (ChPT). Special attention is devoted to one-loop corrections, η - η' mixing effects and vector-meson dominance of ChPT counter-terms. The less interesting $\eta \rightarrow \pi^+\pi^-\gamma\gamma$ transition is briefly discussed too.

The rare decay modes $\eta \rightarrow \pi^0 \pi^0 \gamma \gamma$ and $\eta \rightarrow \pi^+ \pi^- \gamma \gamma$ have been recently discussed by several authors in the context of Chiral Perturbation Theory (ChPT) [1]. A lowest order analysis, i.e. at tree-level in ChPT, has been performed for both decays by Knöchlein, Scherer and Drechsel [2]. More recently, Bellucci and Isidori [3] have extended the analysis for the neutral mode to one-loop in ChPT. When that reference appeared we had finished our analytical work. Preliminary results of this work were presented in [4]. The potential interest of these rare decays is in view of the large number of η 's to be produced in a near future by several facilities. Moreover, the necessity of computing the large one-loop corrections can be traced to the closely related analysis for $\gamma \gamma \rightarrow 3\pi$ [5], as it has been anticipated [3, 4] and fully confirmed in this work and other recent results[3].

We would like to add that our previous computation and discussion of the $\eta \rightarrow \pi^0 \gamma \gamma$ amplitude in ChPT [6] is also particularly illustrating when computing $\eta \rightarrow \pi^0 \pi^0 \gamma \gamma$. Indeed, the observation in [6] that the main contribution to $A(\eta \rightarrow \pi^0 \gamma \gamma)$ comes from the vector meson dominated (VMD) counter-terms of the ChPT Lagrangian, strongly suggests the possibility of similar important contributions to $A(\eta \rightarrow \pi^0 \pi^0 \gamma \gamma)$. The main purpose of the present note is to reconsider the $\eta \rightarrow \pi^0 \pi^0 \gamma \gamma$ decay including this contribution and refining some of the findings in refs.[2, 3]. The $\eta \rightarrow \pi^+ \pi^- \gamma \gamma$ amplitude will be briefly discussed too.

Our notation follows closely that in refs.[5, 6, 7, 8] to which we refer for details. In this notation and for later use, we quote a few relevant amplitudes involving vertices from the lowest-order piece of the ChPT lagrangian, $\mathcal{L}^{(2)}$,

$$\begin{aligned} A(\eta_8 \rightarrow \pi^0 \pi^0 \pi^0) &= -B(m_d - m_u)/\sqrt{3}f^2 = -2\Delta m_K^2/\sqrt{3}f^2 \\ A(\pi^+(p_+) \pi^-(p_-) \rightarrow \pi^0(p_1) \pi^0(p_2)) &= 2(s_{\pi\pi} - m_\pi^2)/f^2, \end{aligned} \quad (1)$$

where $s_{\pi\pi} \equiv (p_+ + p_-)^2 = (p_1 + p_2)^2 = p_{12}^2$, $f_\pi \simeq f = 132$ MeV, and $\Delta m_K^2 \simeq 6.2 \times 10^{-3} \text{ GeV}^{-2}$ is the non-photonic contribution to the kaon mass difference (see [6]). Other useful amplitudes involving vertices of the anomalous sector of the ChPT lagrangian, $\mathcal{L}_{WZ}^{(4)}$, are, e.g.,

$$\begin{aligned} A(\pi^0 \rightarrow \gamma(k_1) \gamma(k_2)) &= \sqrt{3}A(\eta_8 \rightarrow \gamma \gamma) = \frac{-\sqrt{2}e^2}{4\pi^2 f} \epsilon_{\mu\nu\alpha\beta} \epsilon_1^\mu k_1^\nu \epsilon_2^\alpha k_2^\beta \\ A(\eta_8(p_3) \rightarrow \pi^+(p_+) \pi^-(p_-) \gamma) &= \frac{e}{\sqrt{6}\pi^2 f^3} \epsilon_{\mu\nu\alpha\beta} \epsilon^\mu p_3^\nu p_+^\alpha p_-^\beta. \end{aligned} \quad (2)$$

The use of VMD to estimate counter-terms of the anomalous sector of the ChPT lagrangian (see ref.[7]) requires the introduction of effective lagrangians such as

$$\mathcal{L}_{VVP} = G/\sqrt{2} \epsilon_{\mu\nu\alpha\beta} \text{tr}(\partial^\mu V^\nu \partial^\alpha V^\beta P)$$

and

$$\mathcal{L}_{V\gamma} = -2egf^2 A^\mu \text{tr}(QV_\mu) = -eM_{\rho,\omega}^2/\sqrt{2}g(\rho_\mu^0 A^\mu + \frac{1}{3}\omega_\mu A^\mu - \frac{\sqrt{2}}{3}\phi_\mu A^\mu)$$

accounting for the VVP and $V\gamma$ transitions with $M_\rho^2 \simeq M_\omega^2 = 2g^2 f^2$ and $g \simeq 4.15$ [7, 8]. From these lagrangians one obtains a series of $SU(3)$ -related amplitudes such as

$$\begin{aligned} A(\omega \rightarrow \rho^0 \pi^0) &= \sqrt{3} A(\omega \rightarrow \omega \eta_8) = G \epsilon_{\mu\nu\alpha\beta} \epsilon_i^\mu p_i^\nu \epsilon_f^\alpha p_f^\beta \\ A(\omega \rightarrow \pi^0 \gamma) &= 3A(\rho \rightarrow \pi \gamma) = \frac{eG}{\sqrt{2}g} \epsilon_{\mu\nu\alpha\beta} \epsilon_i^\mu p_i^\nu \epsilon_f^\alpha k^\beta, \end{aligned} \quad (3)$$

which allows one to recover the whole standard VMD phenomenology and, in particular, the previous amplitudes (2) for $\pi^0, \eta_8 \rightarrow \gamma\gamma$ if $G = 3\sqrt{2}g^2/4\pi^2 f$.

The treatment in ChPT of the physical η -particle, resulting from the mixing between the octet and singlet states η_8 and η_1 , is not a trivial subject and deserves special attention, as recently emphasized by Leutwyler and others [9, 10]. Following these references and previous phenomenological work in refs [6, 7], we are going to distinguish between radiative vertices related to the anomalous part of the lagrangian, $\mathcal{L}_{WZ}^{(4)}$, and the non-anomalous ones coming from $\mathcal{L}^{(2)}$ and $\mathcal{L}^{(4)}$. In the latter case, only the $SU(3)$ octet of Goldstone bosons are considered to appear in $\mathcal{L}^{(2)}$ and the whole effect of the octet-singlet mixing is assumed to proceed through the L_7^r counter-term of the next order piece of the lagrangian, $\mathcal{L}^{(4)}$ [1, 9, 10]. As it is suggested in [10], however, the situation can be different for the radiative vertices contained in $\mathcal{L}_{WZ}^{(4)}$. Indeed, a satisfactory description of $\eta \rightarrow \gamma\gamma$ and $\eta \rightarrow \pi^+ \pi^- \gamma$ can only be achieved [7, 12] by introducing the phenomenological $\eta - \eta'$ mixing angle, $\theta \simeq -19.5^\circ$ [13], and extending from the $SU(3)$ -octet to the $U(3)$ -nonet the fields appearing in $\mathcal{L}_{WZ}^{(4)}$. In this extended nonet-symmetric context one then has $A(\eta_1 \rightarrow \gamma\gamma) = 2\sqrt{2}A(\eta_8 \rightarrow \gamma\gamma)$, $A(\eta_1 \rightarrow \pi^+ \pi^- \gamma) = \sqrt{2}A(\eta_8 \rightarrow \pi^+ \pi^- \gamma)$, $A(\rho \rightarrow \eta_1 \gamma) = \sqrt{2}A(\rho \rightarrow \eta_8 \gamma)$, and other similarly simple relations for anomalous vertices.

Once we have fixed all the above couplings, the computation of the $\eta \rightarrow \pi^0 \pi^0 \gamma\gamma$ amplitude in ChPT is a straightforward task. For convenience we will consider four separate contributions to the amplitude

$$\begin{aligned} A(\eta \rightarrow \pi^0 \pi^0 \gamma\gamma) &\equiv A(\eta(p_3) \rightarrow \pi^0(p_1) \pi^0(p_2) \gamma(k_1) \gamma(k_2)) \\ &= A(\eta \rightarrow \pi^0 \pi^0 \gamma\gamma)_{\pi^0\text{-pole}} + A(\eta \rightarrow \pi^0 \pi^0 \gamma\gamma)_{\eta\text{-tail}} \\ &+ A(\eta \rightarrow \pi^0 \pi^0 \gamma\gamma)_{1PI} + A(\eta \rightarrow \pi^0 \pi^0 \gamma\gamma)_{VMD}. \end{aligned} \quad (4)$$

The first two correspond to one-particle reducible diagrams containing the π^0 or η propagator and will be computed up to one-loop, i. e., at $O(p^4)$ and $O(p^6)$ in ChPT, as in ref.[3]. The third term corresponds to one-particle irreducible (1PI) diagrams and completes the one-loop calculation, $O(p^6)$ in ChPT. The final term contains the VMD contributions to the low energy constants or counter-terms of the ChPT Lagrangian at order p^8 and higher, but their effects are not necessarily negligible, as the analysis of $\eta \rightarrow \pi^0 \gamma\gamma$ in [6] indicates.

Most of the $\eta \rightarrow \pi^0 \pi^0 \gamma\gamma$ decay events are expected to proceed through the $\eta \rightarrow \pi^0 \pi^0 \pi^0 \rightarrow \pi^0 \pi^0 \gamma\gamma$ decay chain, having to do with the well-studied, isospin-violating $\eta \rightarrow 3\pi^0$ decay amplitude [1, 10], rather than being genuine $\eta \rightarrow \pi^0 \pi^0 \gamma\gamma$ decays. A convenient way to write the ChPT amplitude for this kind of background is

$$A(\eta \rightarrow \pi^0 \pi^0 \gamma\gamma)_{\pi^0\text{-pole}} = \frac{-e^2}{\sqrt{6}\pi^2 f_\pi^3} \frac{\Delta m_K^2}{s - m_\pi^2 + im_\pi \Gamma_\pi} \epsilon_{\mu\nu\alpha\beta} \epsilon_1^\mu k_1^\nu \epsilon_2^\alpha k_2^\beta$$

$$\times(1+U+V+W)\left(1+\frac{1}{3}\frac{m_\pi^2}{m_\eta^2-m_\pi^2}-\frac{1}{3}\frac{m_\pi^2}{m_\eta^2-s}\right), \quad (5)$$

where $s \equiv s_{\gamma\gamma} = (k_1 + k_2)^2$ and the final factor has been included to account for the off-shellness of the π^0 in one of the three possible $\pi^0 \rightarrow \gamma\gamma$ transitions, but can be safely neglected. Taking $U = V = W = 0$ and $f_\eta = f_\pi = f$ in the above amplitude corresponds to the $O(p^4)$ tree-level result. Sizeable loop corrections and η - η' effects are included following refs. [1, 10]. For the former we simplify our analysis (see ref. [14]) taking $U + V = 0.39 - 0.03 + 0.18i$, as corresponds to the center of the $\eta \rightarrow 3\pi^0$ Dalitz plot [1]. The η - η' mixing effects are parametrized taking $1 + W \simeq 1 + \frac{2}{3}\Delta_{GMO} \simeq 1.15$ in agreement with the value given in [1, 10], but somewhat below $1 + W \simeq \sqrt{2}$ coming from nonet-symmetry arguments with $\theta \simeq -19.5^\circ$. With these values and $\Delta m_K^2 \simeq 6.2 \times 10^{-3} \text{ GeV}^2$ one obtains $\Gamma(\eta \rightarrow 3\pi^0) = 315 \text{ eV}$, reasonably close to the experimental value $\Gamma(\eta \rightarrow 3\pi^0)_{exp} = 379 \pm 36 \text{ eV}$ [11]. Using eq.(5) one also obtains the dashed curve plotted in Fig. 1, clearly showing the π^0 -pole in the $\gamma\gamma$ mass spectrum. Both this result and the above discussion are essentially equivalent to those presented in ref.[3], except for a possible sign (see below) of no relevance here and the value for $(1 + U + V + W) \simeq \rho = 2$ which in [3] is taken from the experimental $\eta \rightarrow 3\pi^0$ decay width.

Another independent contribution to $\eta \rightarrow \pi^0\pi^0\gamma\gamma$ proceeds through the isospin conserving decay chain $\eta \rightarrow \pi^0\pi^0\eta \rightarrow \pi^0\pi^0\gamma\gamma$. The corresponding ChPT amplitude at one-loop can be written as

$$\begin{aligned} A(\eta \rightarrow \pi^0\pi^0\gamma\gamma)_{\eta\text{-tail}} &= \frac{e^2}{12\sqrt{6}\pi^2 f_\pi^2 f_\eta} \frac{m_\pi^2}{s - m_\eta^2} (1 + C_{loops}) (\cos\theta - 2\sqrt{2}\sin\theta) \\ &\times \epsilon_{\mu\nu\alpha\beta} \epsilon_1^\mu k_1^\nu \epsilon_2^\alpha k_2^\beta + \begin{pmatrix} k_1 \\ \epsilon_1 \end{pmatrix} \leftrightarrow \begin{pmatrix} k_2 \\ \epsilon_2 \end{pmatrix} + (p_1 \leftrightarrow p_2) + \dots, \end{aligned} \quad (6)$$

where the angular factor $\cos\theta - 2\sqrt{2}\sin\theta \simeq 4\sqrt{2}/3$ takes into account both the η_8 and $\eta_1 \rightarrow \gamma\gamma$ radiative decays thus justifying the use of the physical η mass in the propagator. The dots stand for negligible contributions involving an η' propagator. As previously discussed, the treatment of η - η' mixing for the initial η —coupled to $\pi^0\pi^0\eta$ through the mass terms in $\mathcal{L}^{(2)}$ — is different and leads to the factor $(1 + C_{loops})$ in the above amplitude where, apart from the tree-level contribution, the loop effects are included in C_{loops} . They are explicitly given in the Appendix and contain η - η' mixing effects in the L_γ^r counter-term [10]. A more sophisticated analysis of this contribution to $\eta \rightarrow \pi^0\pi^0\gamma\gamma$ seems unnecessary since its numerical effects, as also observed in [3], are found to be rather small.

A more genuine contribution to $\eta \rightarrow \pi^0\pi^0\gamma\gamma$ involves pion loops (as well as numerically less important kaon, η and $\pi\eta$ loops) with an $\eta \rightarrow \pi^+\pi^-\gamma(\gamma)$ anomalous vertex from $\mathcal{L}_{WZ}^{(4)}$ followed by $\pi^+\pi^-(\gamma) \rightarrow \pi^0\pi^0\gamma$ rescattering. As expected this is an important correction. The reason is that, contrary to the tree-level amplitudes, this $O(p^6)$ contribution does not vanish in the chiral limit. Indeed, restricting for the moment to the octet piece of the physical η , we find

$$\begin{aligned}
A(\eta_8 \rightarrow \pi^0 \pi^0 \gamma \gamma)_{1PI}^{\pi\text{-loops}} &= \frac{-4e^2(m_\pi^2 - p_{12}^2)}{\sqrt{6}\pi^2 f_\pi^2 f_\eta} \frac{1}{16\pi^2 f^2} \\
&\times R(p_{12}^2, -k \cdot p_{12}, m_\pi^2) \epsilon_{\mu\nu\alpha\beta} (-\epsilon_1^\mu + \frac{\epsilon_1 \cdot p_{12}}{k_1 \cdot p_{12}} k_1^\mu) k_2^\nu p_3^\alpha \epsilon_2^\beta + \left[\begin{pmatrix} k_1 \\ \epsilon_1 \end{pmatrix} \leftrightarrow \begin{pmatrix} k_2 \\ \epsilon_2 \end{pmatrix} \right],
\end{aligned} \tag{7}$$

where the function R is defined in the Appendix. This result—which is pivotal in the whole discussion—fully agrees with the expression obtained by Bellucci and Isidori (BI) [3].

However, when eq.(7) is combined with the previous π^0 -pole and η -tail amplitudes, eqs.(5,6), we disagree in the interference pattern. While in [3], there is constructive interference in the interval $0.08 \leq z \equiv m_{\gamma\gamma}^2/m_\eta^2 < 0.25$, we obtain a destructive one. We believe that the origin of this discrepancy is a different, relative sign between our π^0 -pole contribution (5) and the corresponding one in ref.[3], once the two notations have been unified. In Fig. 1 we plot (solid line) the di-photon mass spectrum obtained adding our eqs.(5) and (7). To approximately reproduce the results by BI [3], we simply have to reverse the sign of our eq.(5). The resulting curve is also plotted (upper dotted line) in Fig. 1.

Up to this point, in this 1PI contribution there has been no discussion on the effects of η - η' mixing, which, as previously mentioned, are required to correctly describe the $\eta \rightarrow \pi^+ \pi^- \gamma(\gamma)$ vertices [12] appearing in the 1PI one-loop diagrams. Restricting to the dominant pion loops, the η - η' mixing effects translate simply into the following enhancement in the amplitude for the physical η

$$\begin{aligned}
A(\eta \rightarrow \pi^0 \pi^0 \gamma \gamma)_{1PI}^{\pi\text{-loops}} &= (\cos \theta - \sqrt{2} \sin \theta) \times A(\eta_8 \rightarrow \pi^0 \pi^0 \gamma \gamma)_{1PI}^{\pi\text{-loops}} \\
&\simeq \sqrt{2} A(\eta_8 \rightarrow \pi^0 \pi^0 \gamma \gamma)_{1PI}^{\pi\text{-loops}}.
\end{aligned} \tag{8}$$

For completeness, we have also computed kaon and $\pi\eta$ loop effects confirming that they are small compared to the dominant one from pion loops, as also found in [3] for the kaon loops ($\pi\eta$ loops were neglected there). The complete expressions for the η -tail and 1PI amplitudes at $O(p^6)$ are given in the Appendix. Notice the presence of the mixing angle θ and the low-energy constant L_7^r in our result for the η -tail amplitude. This is not double-counting the mixing effects, but it is due to our treatment for the η - η' mixing, using explicitly the angle θ in the radiative transitions and L_7^r in the non-anomalous vertices involving four pseudoscalars. The rest of L_i^r counter-terms are needed to obtain a finite result, which turns out to be rather insensitive to their actual values. We show in Fig. 2 the di-photon spectrum corresponding to our $O(p^6)$ result, taking $f_\pi \simeq f$ and $f_\eta \simeq 1.3f_\pi$ (upper dotted line). It turns out that these complete one-loop amplitude dominates over the π^0 -pole background alone for $z < m_\pi^2/m_\eta^2$ (at the left-hand side of the pion-pole) and also for $z > 0.17$. (This result contrasts again with the one obtained by BI.)

At this point, one can wonder about the importance of next-next-to leading corrections. This corresponds to $O(p^8)$ in the chiral counting and its complete computation is out of the scope of the present work. It would involve two-loop diagrams with one vertex

from $\mathcal{L}_{WZ}^{(4)}$ and the rest from $\mathcal{L}^{(2)}$; one-loop diagrams with either one vertex from $\mathcal{L}_{WZ}^{(6)}$ and the rest from $\mathcal{L}^{(2)}$ or with the presence of vertices from $\mathcal{L}_{WZ}^{(4)}$ and $\mathcal{L}^{(4)}$; and also $O(p^8)$ tree-level diagrams. The latter can be estimated through VMD, which can also be viewed as a full all-order estimate of the counter-terms, as discussed in [6] for the process $\eta \rightarrow \pi^0 \gamma \gamma$. Computing the VMD diagrams with two vector meson propagators and using amplitudes like those in eq.(3), one obtains

$$\begin{aligned}
A(\eta \rightarrow \pi^0 \pi^0 \gamma \gamma)_{VMD} = & \frac{e^2 G^3}{\sqrt{6} g^2} (1 + \frac{1}{9}) \epsilon_{\rho\alpha\beta\gamma} \epsilon_{\lambda\sigma}{}^{\rho\omega} \epsilon_{\mu\nu\tau\omega} \epsilon_2^\alpha k_2^\beta (p_1 + k_1)^\lambda \epsilon_1^\mu k_1^\nu p_1^\tau \\
& \left(\frac{1}{m_V^2 - (p_3 - k_2)^2} \frac{1}{m_V^2 - (p_1 + k_1)^2} p_3^\gamma p_2^\sigma \right. \\
& + \frac{1}{m_V^2 - (p_1 + k_1)^2} \frac{1}{m_V^2 - (p_2 + k_2)^2} p_2^\gamma p_3^\sigma \Big) \\
& + \left[\begin{pmatrix} k_1 \\ \epsilon_1 \end{pmatrix} \leftrightarrow \begin{pmatrix} k_2 \\ \epsilon_2 \end{pmatrix} \right] + (p_1 \leftrightarrow p_2), \tag{9}
\end{aligned}$$

In Fig. 2 we show (lower dotted curve) the di-photon invariant mass spectrum corresponding to this VMD amplitude alone. Integrating over the whole spectrum leads to $\Gamma_{VMD}(\eta \rightarrow \pi^0 \pi^0 \gamma \gamma) \simeq 3.2 \times 10^{-6}$ eV, not far from old VMD estimates [15]. Our final result, containing the four contributions listed in eq.(4), is also plotted (solid line) in Fig. 2 and can be compared with our previous full amplitude at order p^6 (upper dotted line). The higher order VMD contribution decreases (increases) the order- p^6 amplitude in the large (narrow) region of the $\gamma\gamma$ -spectrum above (below) the π^0 -pole. We predict a rather small $\eta \rightarrow \pi^0 \pi^0 \gamma \gamma$ decay width for $z \simeq 1/4$, but the possibility of observing a departure from the dominant π^0 -pole background (dashed line in Figs.1 and 2) due to chiral-loop and vector-meson effects seems clearly open in the range $0.08 < z < 0.18$.

As in our previous analysis on $\eta \rightarrow \pi^0 \gamma \gamma$, we have now achieved a rather complicated description for the closely related $\eta \rightarrow \pi^0 \pi^0 \gamma \gamma$ amplitude, containing various contributions whose relative weights are difficult to disentangle. To clarify this issue and to test our results, we have computed analytically these separate contributions at the higher end of the $\gamma\gamma$ -spectrum, $z \simeq 1/4$ if one takes $m_\eta \simeq 4m_{\pi^0} \equiv 4m$. Here, the two γ 's fly apart with the same helicities and energies, $E_\gamma \simeq m$. Working with $\eta \rightarrow \pi^0 \pi^0 \gamma \gamma$ helicity amplitudes one thus obviously has $A^{+-} = A^{-+} = 0$ and $A^{++} = A^{--}$. For the latter, our four eqs.(5,6,8,9) imply the following four contributions displayed according to the decomposition in eq.(4),

$$\begin{aligned}
A^{\pm\pm} & \simeq \frac{\sqrt{2}}{9\sqrt{3}} \frac{e^2 m^2}{\pi^2 f_\pi^2 f_\eta} \left\{ -(1 + U + V + W) \frac{f_\eta}{f_\pi} - 0.5(1 + C_{loops}) - 3.9 \frac{m^2}{f^2} R + 0.20 \frac{f_\eta}{f_\pi} \left(\frac{g}{\pi} \right)^4 \right\} \\
& \simeq \frac{\sqrt{2}}{9\sqrt{3}} \frac{e^2 m^2}{\pi^2 f_\pi^2 f_\eta} \left\{ -(1.51 + 0.18i) \frac{f_\eta}{f_\pi} - 0.1 + (1.4 - 3.1i) + 0.81 \right\}, \tag{10}
\end{aligned}$$

where the following approximations have been made: $\Delta m_K^2 \simeq m^2/3$, $M_V = M_{\rho,\omega}^2 \simeq 33m^2$ and $R \equiv R(4m^2, -2m^2, m^2) \simeq -0.36 + 0.84i$. In this same spirit, we have worked out

an approximate expression for the diphoton spectrum, valid for $z \rightarrow 1/4$, i.e., for non-relativistic pions, which serves to fix the global normalization. We find

$$\left. \frac{d\Gamma(\eta \rightarrow \pi^0 \pi^0 \gamma \gamma)}{dz} \right|_{z \simeq 1/4} \simeq \frac{\sqrt{2} m^3}{(4\pi)^4} (|A^{++}|^2 + |A^{--}|^2) \frac{z^{1/4} (1 - 2m/m_\eta^{exp} - \sqrt{z})^2}{(1 + 2\sqrt{z})^{3/2}}, \quad (11)$$

where the experimental value of the η -mass, m_η^{exp} , has been kept in the final factor of the phase-space term in order to get a reliable result at the end of the spectrum. We can then approximately reproduce all our results in Figs.1 and 2 for $z \rightarrow 1/4$, as it is shown by the symbols (diamonds) at the end of the spectrum, corresponding to the π^0 -pole (Fig. 1) and the total (Fig. 2) contributions.

We now turn to briefly discuss the charged channel $\eta \rightarrow \pi^+ \pi^- \gamma \gamma$. The isospin conserving, tree level matrix element is simply found to be

$$\begin{aligned} A(\eta_8 \rightarrow \pi^+ \pi^- \gamma \gamma) &= \frac{e^2}{\sqrt{6} f^3 \pi^2} \epsilon_{\mu\nu\alpha\beta} \epsilon_1^\mu k_1^\nu \left(\frac{1}{6} \frac{m_\pi^2}{s - m_\eta^2} \epsilon_2^\alpha k_2^\beta \right. \\ &\quad \left. + (\epsilon_2^\alpha + \frac{p_+ \cdot \epsilon_2}{p_+ \cdot k_2} p_-^\alpha + \frac{p_- \cdot \epsilon_2}{p_- \cdot k_2} p_+^\alpha) p_3^\beta \right) + \left[\begin{pmatrix} k_1 \\ \epsilon_1 \end{pmatrix} \leftrightarrow \begin{pmatrix} k_2 \\ \epsilon_2 \end{pmatrix} \right], \quad (12) \end{aligned}$$

as in the analysis by Knöchlein et al. [2]. This amplitude contains two independent, gauge invariant pieces, similar to those entering the $\gamma\gamma \rightarrow \pi^+ \pi^- \pi^0$ amplitude [5]. In the latter process, these two pieces tend to cancel due to an almost perfect destructive interference and thus making the next $O(p^6)$ corrections—which spoil the previous almost perfect cancellation— numerically very important. Instead, in the tree-level η_8 decay amplitude (12), the second piece—which corresponds to a brehmstrahlung process—is singular for vanishing photon energies, and thus dominates over the former. Thanks to this, in order to compute $O(p^6)$ corrections, one can reasonably restrict oneself only to those corresponding to the dominant bremsstrahlung piece, which can easily be obtained applying Low theorem to the $O(p^6)$ contribution for $\eta \rightarrow \pi^+ \pi^- \gamma$ [12]. In addition, one also has to include the isospin violating contribution, mediated by a π^0 pole via the decay chain $\eta \rightarrow \pi^+ \pi^- \pi^0 \rightarrow \pi^+ \pi^- \gamma \gamma$, which can be estimated, at $O(p^6)$ and including η - η' - mixing effects, along the same lines as in the neutral channel.

In Fig. 3 we show the di-photon mass spectrum for the $\eta \rightarrow \pi^+ \pi^- \gamma \gamma$ decay at $O(p^6)$ (solid line); the tree-level prediction for the $\eta_8 \rightarrow \pi^+ \pi^- \gamma$ process is also shown (dashed line). The latter is in reasonable agreement with the results in ref. [2]. The former represents a substantial correction to (it is ~ 3 times larger than) the tree-level result, as should be expected from the dynamics of the underlying $\eta \rightarrow \pi^+ \pi^- \gamma$ transition. Indeed, from its analysis in ref. [12] one immediately can deduce that $\Gamma(\eta_8 \rightarrow \pi^+ \pi^- \gamma)_{tree-level} \simeq (1/3) \Gamma(\eta \rightarrow \pi^+ \pi^- \gamma)_{one-loop}$. The nice interference pattern in Fig. 3 corresponds to the π^0 pole entering the isospin violating amplitude. But all these results refer essentially to the dynamics of the $\eta \rightarrow \pi^+ \pi^- \gamma$ and $\eta \rightarrow \pi^+ \pi^- \pi^0$ amplitudes rather than being genuine $\eta \rightarrow \pi^+ \pi^- \gamma \gamma$ dynamical effects. The latter will be very hard to disentangle from this dominant background. In this sense, we agree with BI [3] in that a more detailed

calculation seems unnecessary. Unsuccessful experimental attempts to detect $\eta \rightarrow \pi^+\pi^-\gamma\gamma$ decay events can be found in ref.[16].

In summary, while the $\eta \rightarrow \pi^+\pi^-\gamma\gamma$ process seems scarcely interesting from the point of view of ChPT, the situation looks very different for the neutral $\eta \rightarrow \pi^0\pi^0\gamma\gamma$ decay mode. Although the partial width is predicted to be rather small, chiral-loop and VMD-counterterm effects could be detected and analyzed. This same qualitative conclusion has also been reached by other recent ChPT analyses.

ACKNOWLEDGEMENTS

This work has been supported by CICYT, AEN95-815 and by the EURODAFNE, HCMP, EEC contract # CHRX-CT920026. P.T. has been supported by the EU TMR program under contract number ERB 4001GT952585.

Appendix

In this Appendix we quote the complete $O(p^6)$, isospin conserving matrix element for $\eta \rightarrow \pi^0 \pi^0 \gamma \gamma$. The isospin violating contribution (the background) proceeds through a π^0 pole and is written in eq.(5) in the text.

$$\begin{aligned}
A(\eta(p_3) \rightarrow \pi^0(p_1)\pi^0(p_2)\gamma(k_1)\gamma(k_2))_{1PI}^{one-loop} &= \frac{-e^2}{\sqrt{6}\pi^2 f_\pi^2 f_\eta} \frac{1}{16\pi^2 f^2} \epsilon_{\mu\nu\alpha\beta} \\
&\left(\cos\theta(4m_K^2 - 3p_{13}^2)R(p_{13}^2, -k_1 \cdot p_{13}, m_K^2)(-\epsilon_1^\mu + \frac{\epsilon_1 \cdot p_{13}}{k_1 \cdot p_{13}}k_1^\mu)k_2^\nu p_2^\alpha \epsilon_2^\beta \right. \\
&+ \cos\theta(4m_K^2 - 3p_{23}^2)R(p_{23}^2, -k_1 \cdot p_{23}, m_K^2)(-\epsilon_1^\mu + \frac{\epsilon_1 \cdot p_{23}}{k_1 \cdot p_{23}}k_1^\mu)k_2^\nu p_1^\alpha \epsilon_2^\beta \\
&- 2(\cos\theta - \sqrt{2}\sin\theta)\left(\frac{p_{12}^2}{2}R(p_{12}^2, -k_1 \cdot p_{12}, m_K^2) - 2(m_\pi^2 - p_{12}^2)R(p_{12}^2, -k_1 \cdot p_{12}, m_\pi^2)\right) \\
&\left. (-\epsilon_1^\mu + \frac{\epsilon_1 \cdot p_{12}}{k_1 \cdot p_{12}}k_1^\mu)k_2^\nu p_3^\alpha \epsilon_2^\beta \right) + \left[\begin{pmatrix} k_1 \\ \epsilon_1 \end{pmatrix} \leftrightarrow \begin{pmatrix} k_2 \\ \epsilon_2 \end{pmatrix} \right] \Bigg\}, \tag{13}
\end{aligned}$$

$$\begin{aligned}
A(\eta \rightarrow \pi^0 \pi^0 \gamma \gamma)_{\eta \text{ tail}}^{one-loop} &= \frac{e^2}{12\sqrt{6}\pi^2 f_\pi^2 f_\eta} \epsilon_{\mu\nu\alpha\beta} \epsilon_1^\mu k_1^\nu \epsilon_2^\alpha k_2^\beta \\
&\times \left\{ \left(1 + C_{loops}(p_{12}, p_{13}, k_1) \right) \left(\frac{m_\pi^2}{s - m_\eta^2} (\cos\theta - 2\sqrt{2}\sin\theta) + \frac{m_\pi^2}{s - m_{\eta'}^2} 2\sqrt{2}\sin\theta \right) \right. \\
&\left. + (p_{13} \leftrightarrow p_{23}) + \left[\begin{pmatrix} k_1 \\ \epsilon_1 \end{pmatrix} \leftrightarrow \begin{pmatrix} k_2 \\ \epsilon_2 \end{pmatrix} \right] \right\}, \tag{14}
\end{aligned}$$

where C_{loops} contains the $O(p^6)$ loop- and counter-term-contributions which combine into the finite result

$$\begin{aligned}
C_{loops}(p_{12}, p_{13}, k_1) &= \frac{1}{16\pi^2 f^2} \left[4A(m_\pi^2) + \frac{A(m_K^2)}{m_\pi^2} \left(\frac{5}{2}s + \frac{19}{6}m_\pi^2 - \frac{5}{2}p_{12}^2 + \frac{10}{3}m_K^2 - 5p_{13}^2 \right) \right. \\
&+ B(p_{12}^2, m_\pi^2, m_\pi^2)(-m_\pi^2 + 2p_{12}^2) + \frac{p_{12}^2}{4m_\pi^2} B(p_{12}^2, m_K^2, m_K^2)(-9s + 4m_K^2 - 3m_\pi^2 + 9p_{12}^2) \\
&+ \frac{2}{9}B(p_{12}^2, m_\eta^2, m_\eta^2)(-\frac{7}{2}m_\pi^2 + 8m_K^2) + \frac{4}{3}B(p_{13}^2, m_\eta^2, m_\pi^2)m_\pi^2 \\
&+ B(p_{13}^2, m_K^2, m_K^2)(2m_K^2 + 6\frac{m_K^2}{m_\pi^2}s + \frac{3}{2}\frac{p_{13}^2}{m_\pi^2}(-3s + 3p_{13}^2 - m_\pi^2 - 4m_K^2)) \\
&+ 192\frac{\pi^2}{m_\pi^2} \left[4L_1^r(-\frac{m_\pi^2}{3}(2m_\pi^2 + 5p_{12}^2 - 8m_K^2 - 6s) + p_{12}^2(p_{12}^2 - \frac{4}{3}m_K^2 - s)) \right. \\
&\left. + L_2^r(\frac{2}{3}m_\pi^2(4m_\pi^2 + 8m_K^2 + 4s - 10p_{13}^2) + \frac{16}{3}m_K^2(s - p_{13}^2) + 4p_{13}^2(p_{13}^2 - s)) \right] \tag{15}
\end{aligned}$$

$$\begin{aligned}
& + \frac{2}{3}L_3^r\left(\frac{1}{3}m_\pi^2(2m_\pi^2 - 5p_{12}^2 + 16m_K^2 + 10(s - p_{13}^2)) + p_{12}^2(p_{12}^2 - \frac{4}{3}m_K^2 - s) + \frac{8}{3}m_K^2(s - p_{13}^2)\right. \\
& + 2p_{13}^2(p_{13}^2 - s) + \frac{2}{3}L_4^r(m_\pi^2(7m_\pi^2 + 4p_{12}^2 - 22m_K^2 - 6s) + 8m_K^2p_{12}^2) \\
& + \frac{4}{9}L_5^rm_\pi^2(m_\pi^2 - 4m_K^2 - \frac{3}{2}s) + \frac{16}{3}L_6^rm_\pi^2(-m_\pi^2 + 4m_K^2) \\
& \left. + \frac{64}{3}L_7^rm_\pi^2(m_\pi^2 - m_K^2) + 8L_8^rm_\pi^4\right],
\end{aligned}$$

where $p_{12} = p_1 + p_2$, $p_{13} = p_1 - p_3$, $p_{23} = p_2 - p_3$ and $s = (k_1 + k_2)^2$. The functions A , B and R are defined as

$$A(m^2) = -m^2 \ln \frac{m^2}{\mu^2} \quad (16)$$

$$B(p^2, m_1^2, m_2^2) = \left\{ 1 - \frac{1}{2} \log \frac{m_1^2 m_2^2}{\mu^4} + \frac{m_2^2 - m_1^2}{2p^2} \log \frac{m_1^2}{m_2^2} - \frac{1}{p^2} u_+ u_- \log \frac{u_+ + u_-}{u_+ - u_-} \right\}, \quad (17)$$

with $u_\pm = \sqrt{p^2 - (m_1 \pm m_2)^2}$, which, for equal masses, simplifies to

$$B(p^2, m^2, m^2) = 1 + \beta \ln \frac{\beta - 1}{\beta + 1} - \ln \frac{m^2}{\mu^2}, \quad \beta = \sqrt{1 - \frac{4m^2}{p^2}} \quad (18)$$

and

$$\begin{aligned}
R(p^2, k \cdot p, m^2) &= \frac{1}{2} + \left(\frac{1}{2} - \frac{p^2}{4k \cdot p} \right) \left[\beta' \ln \frac{\beta' - 1}{\beta' + 1} - \beta \ln \frac{\beta - 1}{\beta + 1} \right] \\
&+ \frac{m^2}{4k \cdot p} \left[\ln^2 \frac{\beta - 1}{\beta + 1} - \ln^2 \frac{\beta' - 1}{\beta' + 1} \right],
\end{aligned} \quad (19)$$

with $\beta' = \sqrt{1 - \frac{4m^2}{p^2 - 2k \cdot p}}$ and $k^2 = 0$.

One can check that the scale μ appearing in A and B cancels in C_{loops} , as it corresponds to a physical result. The numerical estimation of C_{loops} has been done using the central value of the L_i^r counter-terms listed in [17].

References

- [1] J. Gasser and L. Leutwyler, Nucl. Phys. **B250** (1985) 465, 539 and Ann. Phys. (N.Y.) **158** (1984) 142.
- [2] G. Knöchlein, S. Scherer and D. Drechsel, Phys. Rev. **D53** (1996) 3634.
- [3] S. Bellucci and G. Isidori, hep-ph/9610328.
- [4] J. Bijnens in "Workshop on Physics with the WASA detector" June 1996, preprint TSL/ISV-96-0150.
- [5] P. Talavera et al., Phys. Lett. **B 376** (1996) 186.
- [6] Ll. Ametller, et al., Phys. Lett. **B 276** (1992) 185.
- [7] J. Bijnens, A. Bramon and F. Cornet, Zeit. f. Phys. **C46** (1990) 599;
J. Bijnens, Int. J. Mod. Phys. **A8** (1993) 3045.
- [8] A. Bramon, A. Grau and G. Pancheri, Phys. Lett. **283** (1992) 416, and
The Second Daphne Physics Handbook, edited by L. Maiani, G. Pancheri and N. Paver, INFN-LNF publication 1995, p. 477.
- [9] S. Peris and E. de Rafael, Phys. Lett. **B348** (1995) 539;
P. Herrera-Siklody et al., hep-ph/9610549.
- [10] H. Leutwyler, Phys. Lett. **B374** (1996) 181;
H. Leutwyler, Phys. Lett. **B374** (1996) 163.
- [11] Particle Data Group, Phys. Rev. **D54** (1996) 1.
- [12] J. Bijnens, A. Bramon and F. Cornet, Phys. Lett. **B237** (1990) 488.
- [13] F. Gilman and R. Kauffman, Phys. Rev. **D36** (1987) 2761,
A. Bramon, Phys. Lett. **51B** (1974) 87.
- [14] R. Baur, J. Kambor and D. Wyler, Nucl. Phys. **B460** (1996) 127;
A. Bramon, P. Gosdzinsky and S. Tortosa, Phys. Lett. **B377** (1996) 140.
- [15] A few old papers dealing with $\eta \rightarrow \pi\pi\gamma\gamma$ decays using VMD and
Current Algebra techniques are
J. Dreitlein et al, Phys. Rev. **160** (1967) 1542;
F. Benavent and A. Bramon, An. de Física, **67** (1971) 483; and
V. V. Solovetv and M. V. Terentev, Sov. J. Nucl. Phys. **16** (1973) 82.
- [16] L. R. Price et al, Phys. Rev. Lett. **18** (1967) 1207;
C. Baltay et al, Phys. Rev. Lett. **19** (1967) 1489.
- [17] J. Bijnens, G. Ecker at J. Gasser, The Second Daphne Physics Handbook, edited by
L. Maiani, G. Pancheri and N. Paver, INFN-LNF publication 1995, p. 125.

List of Figures

1	Diphoton mass spectrum for the $\eta \rightarrow \pi^0\pi^0\gamma\gamma$ decay. Partial results.	12
2	Diphoton mass spectrum for the $\eta \rightarrow \pi^0\pi^0\gamma\gamma$ decay. Final results.	13
3	Diphoton mass spectrum for the $\eta \rightarrow \pi^+\pi^-\gamma\gamma$ decay.	14

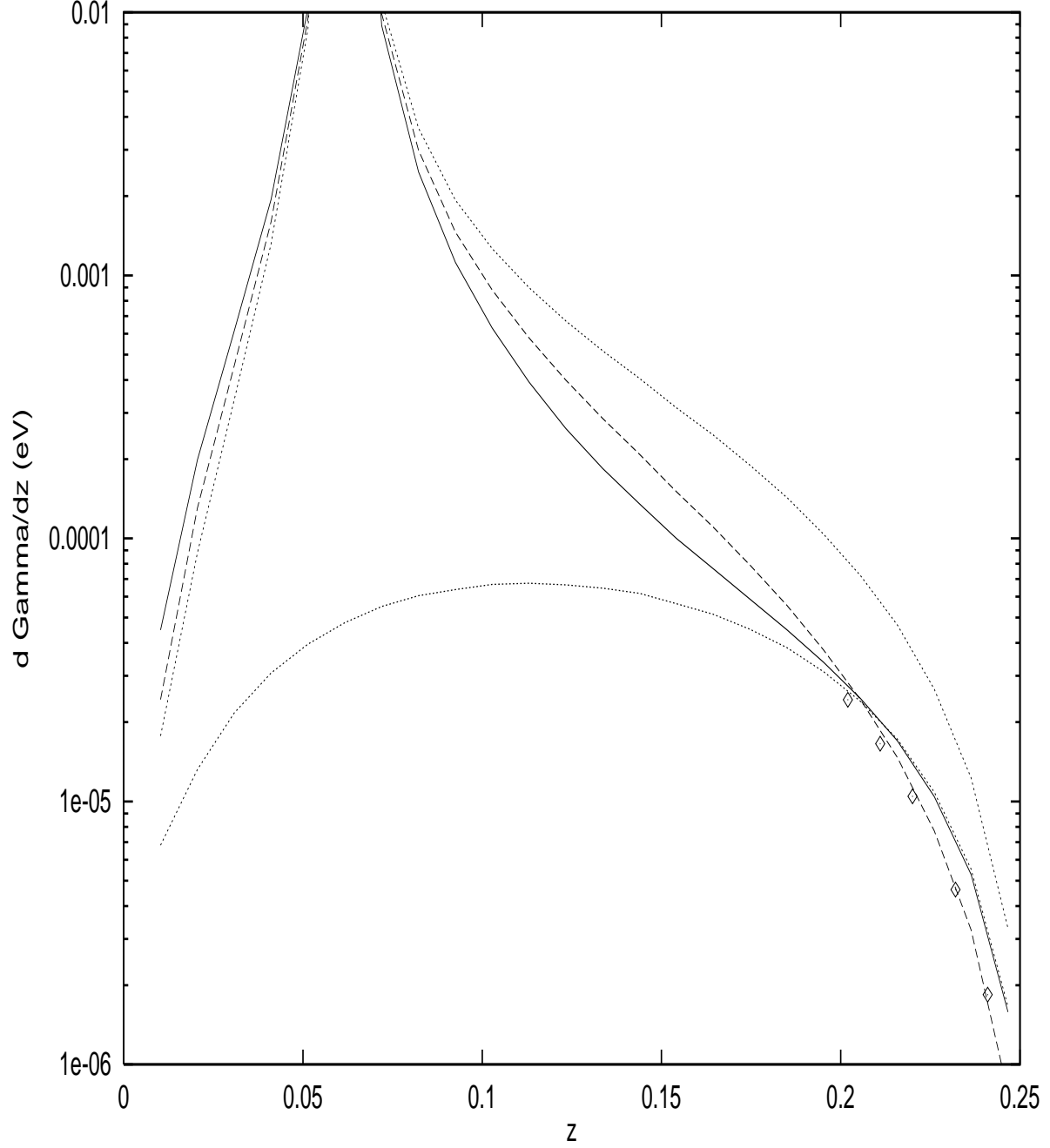


Figure 1: Diphoton mass spectrum for the $\eta \rightarrow \pi^0\pi^0\gamma\gamma$ decay. The dashed line corresponds to the π^0 -pole contribution, eq.(5). The symbols (diamonds) at the end of the spectrum show the π^0 -pole in the approximation of eq.(11) and using the first term of eq.(10). The lowest dotted line is the 1PI result, eq.(7), for η_8 . The solid line is our result when adding eqs.(5) and (7). The upper dotted line (denoted by BI in the text) shows the result of subtracting eqs.(5) and (7).

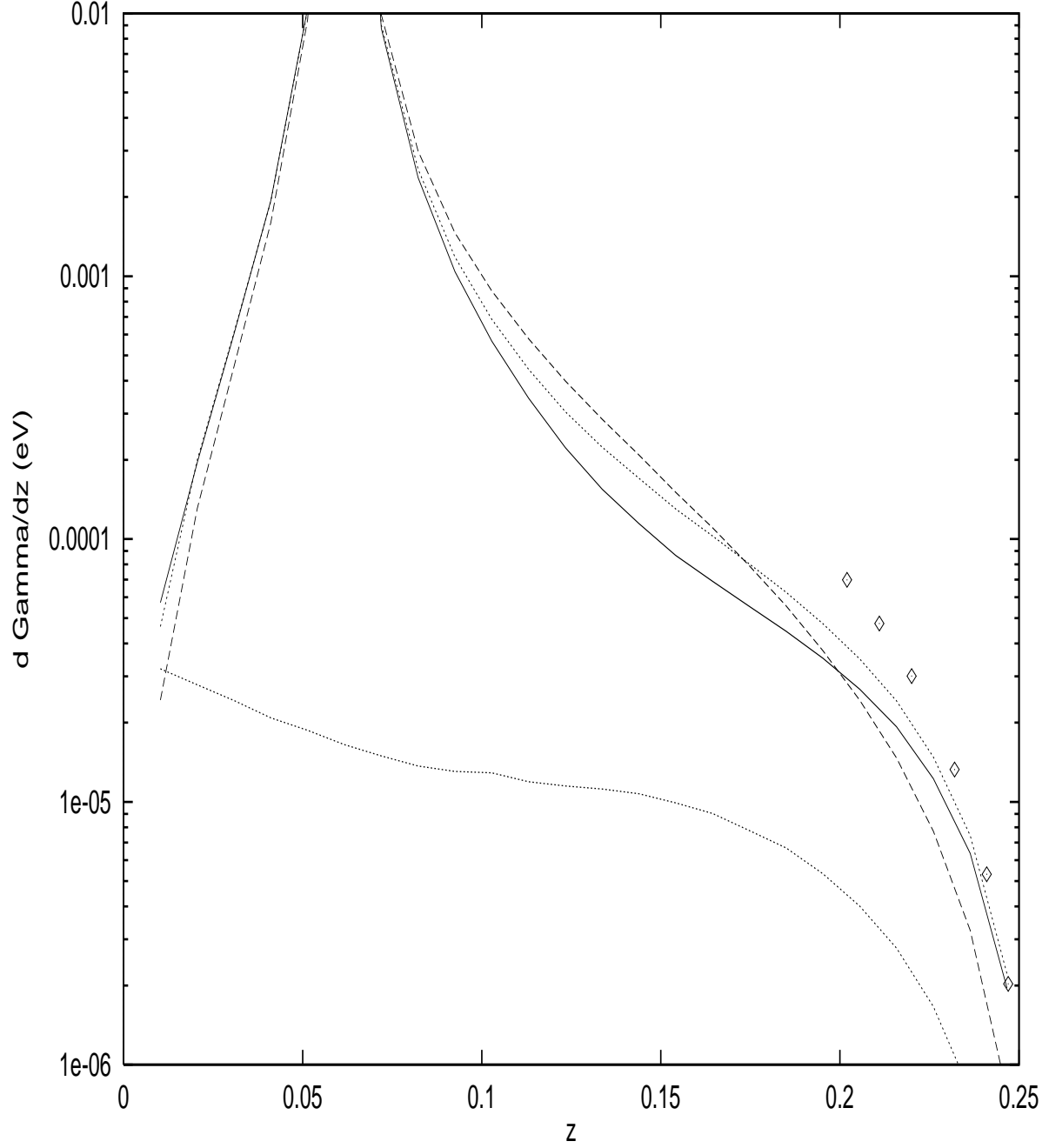


Figure 2: Diphoton mass spectrum for the $\eta \rightarrow \pi^0\pi^0\gamma\gamma$ decay. The dashed line is the π^0 -pole contribution, eq.(5). The upper dotted line corresponds to the $O(p^6)$ result. The lower dotted line is the VMD contribution, eq.(9). The solid line corresponds to the total contribution, listed in eqs.(4,5,6,8 and 9). The symbols (diamonds) at the end of the spectrum show the total result using the approximation of eqs.(10) and (11).

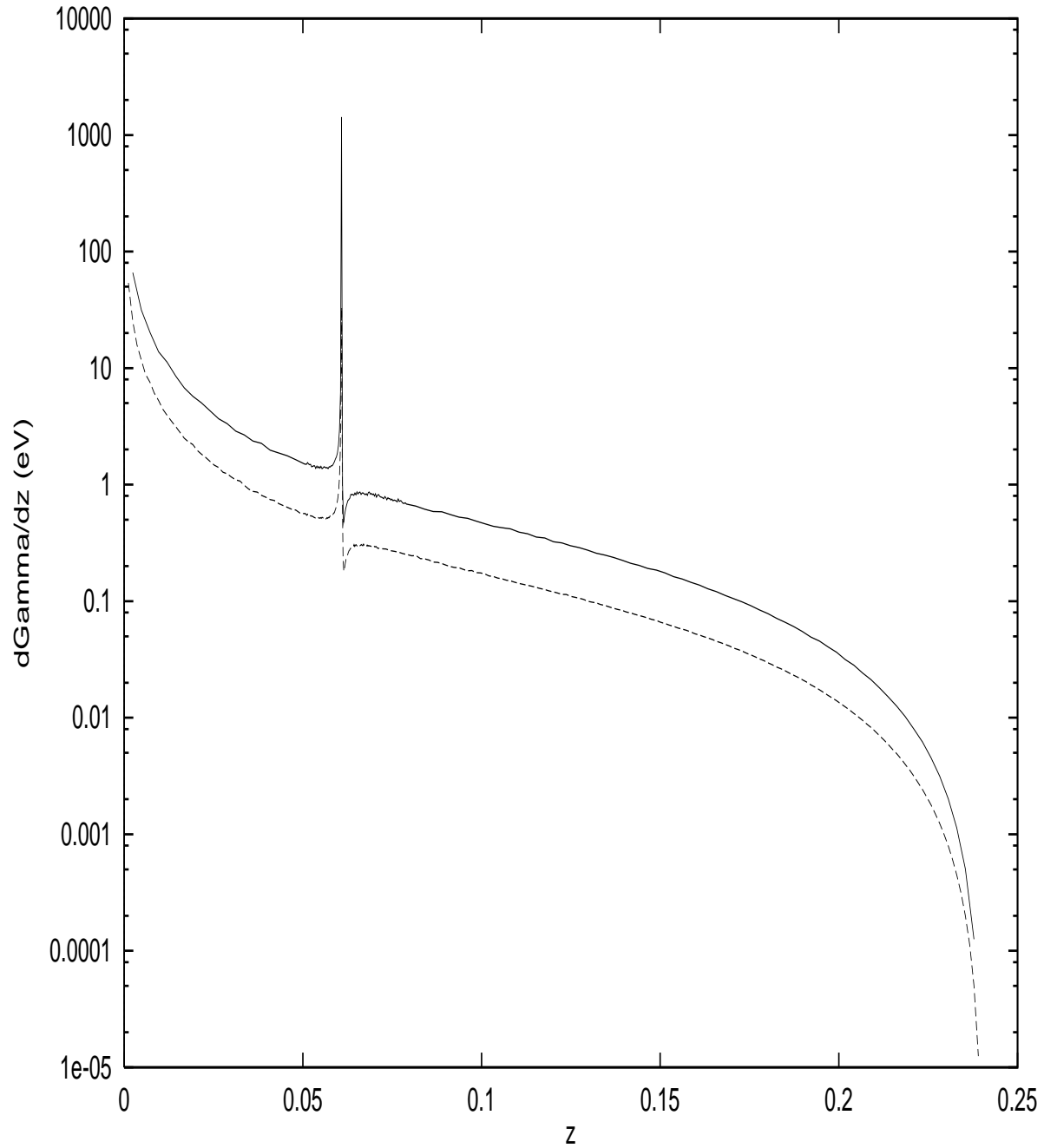


Figure 3: Diphoton mass spectrum for the $\eta \rightarrow \pi^+\pi^-\gamma\gamma$ decay. The solid line is the $O(p^6)$ result. The dashed curve corresponds to the tree-level result for η_8 , eq.(12).